Near Field Probe Measurements in the Plume of a NEXT Ion Thruster

IEPC-2019-167

Presented at the 36th International Electric Propulsion Conference
University of Vienna, Austria
September 15-20, 2019

Neil A. Arthur*
Vantage Partners LLC, Brook Park, OH, 44142, USA

and

George J. Williams†
NASA Glenn Research Center, Cleveland, OH, 44135, USA

Abstract: Due to the extremely long lifetime and ground testing complications, such as facility backpressure effects, modeling is a necessary tool for validating mission lifetime requirements. Both NASA's Glenn Research Center and Jet Propulsion Laboratory have developed lifetime validation models for the NEXT ion thruster. The largest uncertainties in these models are due to unknown plasma properties, such as plasma potential, that occur very near to the grid. Previous studies have made measurements in the mid to far field. Here, very near field measurements of the plasma properties in the ion beam within 0.1 thruster radii of the grid are taken using various probes. Emissive and triple Langmuir probes are swept through the plume to spatially resolve plasma potential, electron temperature and ion density very near to the grid. The goal is to provide refined inputs to the lifetime modeling efforts and increase the accuracy of the models.

Nomenclature

e	= elementary charge
F_{s}	= Screen grid open area fraction
j_{CL}	= Child-Langmuir limited current density
j_{b}	= Beam current density
J_{b}	= Beam current
k_{b}	= Boltzmann constant
ℓ_{a}	= Acceleration length
ℓ_{d}	= Deceleration length
R	= Ratio of net-to-total voltage
r_{t}	= Thruster radius
T_{e}	= Electron temperature
V_{a}	= Accelerator grid voltage
V_{b}	= Beam voltage
V_{N}	= Net accelerating voltage
V_{T}	= Total accelerating voltage

*Aerospace Engineer, Electric Propulsion Systems Branch, neil.arthur@nasa.gov
†Aerospace Engineer, Electric Propulsion Systems Branch, george.j.williams@nasa.gov

I. Introduction

The NEXT ion thruster has an extremely broad throttle range with 40 power levels and demonstrated lifetime in excess of 50 000 h in a ground testing environment.[1] As part of NASA's effort to commercialize and fly the NEXT thruster on various missions, correlating ground demonstrated lifetime to mission specific lifetime predictions is necessary. Missions utilizing ion thrusters may require years of thrusting at varying power levels, therefore life testing for each mission is not feasible and lifetime modeling is necessary.[2] These modeling efforts typically involve simulating erosion of the ion optics, especially the accelerator grid, which is prone to pit and groove erosion.[3–6] The pit and groove erosion is produced by charge-exchange ions which are created when a beam ion strikes a neutral atom. These charge-exchange ions are then accelerated back into the accelerator grid, sputter eroding the grid material. In order to predict the correct magnitude of erosion and also the erosion pattern, the lifetime models need to have information about the potential structure in front of the grid. The potential near the grid is determined by the voltage of the accelerator grid, the density of beam ions, the density of charge-exchange ions, and the density of neutralizer electrons, which interact with the beam ions.

Due to the potentially complex nature of the plasma environment near the ion thruster, the erosion models must be anchored to and validated against test data. Prior measurements have been made for ion thrusters at distances of $\geq$0.1 thruster radii.[7–11] Two companion papers discuss recent modeling efforts, which have identified the largest uncertainties in the models are due to unknown plasma properties at distances of $\leq$0.05 thruster radii.[12,13] This paper discusses plasma property measurements made between 0.02 and 1 thruster radii downstream of the ion optics. Plasma potential, electron temperature, and ion density are measured using emissive and Langmuir probes as a function of both axial and radial distances.

Figure 1: Photographs of probes in VF-16 next to the thruster.

II. Test Setup

Testing occurred at NASA Glenn Research Center in VF-16, which is a 2.75 m diameter by 4.5 m long cylindrical vacuum chamber with a 2×10^{-7} Torr base pressure. The test utilized an engineering model NEXT thruster with a 40 cm diameter beam. Photographs of the setup can be seen in Fig. 1. A rake, depicted in Fig. 2b, including a triple Langmuir probe and six emissive probes, was swept in front of the thruster using a two-axis motion system. Multiple emissive probes were used because their lifetime was very short in the thruster's ion beam.

The probe motion and the coordinate system used in the plots below is shown in Fig. 2a. Due to the fact that the grids are domed for structural purposes, and the probe motion is purely linear, as the probes move towards the edge of the thruster at a given axial distance, the true distance between the probe and the ion optics actually increases. This fact should be noted in interpreting the below data. Position and voltage measurements were taken simultaneously with a data acquisition system to allow for continuous data taking as the probe rake passed through the plume.

The probe tips are at the end of long, thin ceramic tubes, which are mounted on a graphite crossbar. The probes were made to be >30 cm long to reduce the surface area directly in front of the thruster. This

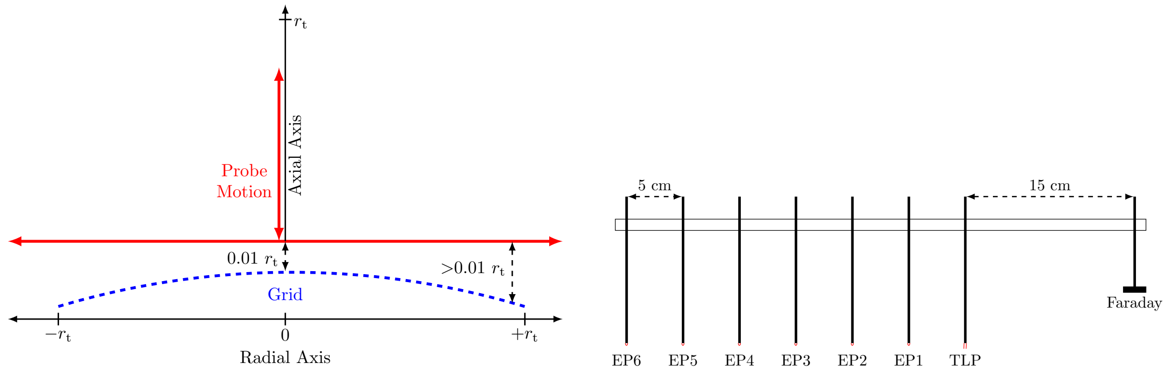

(a) Probe motion and coordinate system.

(b) Probe rake setup showing the six emissive probes, triple Langmuir probe and Faraday probe.

Figure 2: Probe motion coordinate system and probe rake setup. Not to scale.

introduces uncertainty in the probe's radial position that is on the order of 1 mm. The alignment process also has an associated error on the order of 1 mm. A single probe scan generally involved movement in one direction followed immediately by reversing direction along the same path. This was done to determine the thermal effects of the beam on the emissive probes and the perturbation caused by the probes. Probe sweeps were completed in less than 1 min. The measured accelerator current at full power is shown in Fig. 3. The spikes that are a $\sim$30% increase in current are due to the probes passing in front of the thruster, and the spikes to values >25 mA are high voltage recycles. There is a slight upwards trend in accelerator current, as successive probe passes resulted in an increase in current of 10–15%. The discharge properties (current and voltage) were not affected by the prope sweeps.

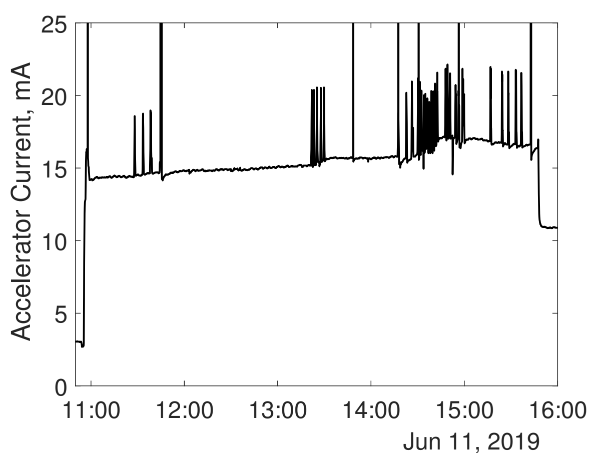

Figure 3: Accelerator current as a function of time while operating at a beam current of 3.52 A and beam voltage of 1800 V.

The plasma potential measured by the emissive probes has an error of approximately $k_b T_e / e$.[14,15] The potential of the emissive probes is measured with respect to facility ground, but in space, the plasma potential relative to the neutralizer cathode is more relavant to the behavior of charge-exchange ions created near the grid. Because it was not feasible to make measurements with respect to the thruster neutralizer and the electron temperature is approximately constant across throttle points, the plots below display normalized plasma potentials. For the purposes of this study, the relative plasma potential trends are the most important. Electron temperatures and ion densities measured using Langmuir probes have an associated error of approximately 25%.[16–18]

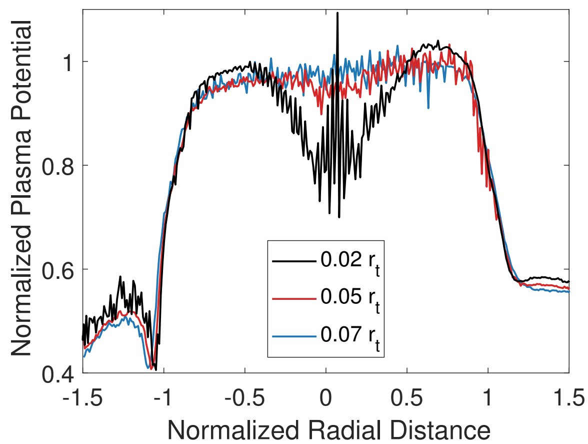

Figure 4: Plasma potential across the front of the thruster at three distances downstream of the optics.

III. Results

A. Plasma Potential

The plasma potential across the face of the thruster for a beam current of 2.7 A and beam voltage of 1179 V is shown in Fig. 4 at three distances from the optics. Unless otherwise noted, all figures present data taken with a single emissive probe. At the closest approach, 0.02 r_{t}, there is a dip in the plasma potential near the thruster centerline. Again, it should be pointed out that the stage motion is such that as the probe nears the edges of the grid it is further from the accelerator surface than it is on centerline. Therefore, the dip may vanish if the probe motion system was able to get very near to the grid at large radii. That said, the radius of curvature of the optics dome is much larger than the radius of the optics themselves, and so near the center of the grid, the probe-to-grid distance is fairly constant. Also, the orientation of the grids is such that the aperture rows are not parallel to the probe motion plane, the aperture rows are angled approximately 10° relative to the horizontal. As the probe moves, it traces across several rows of apertures.

The beam current density measured with a Faraday probe is shown in Fig. 5. From this plot, there is no beam current density peak on centerline that corresponds to the potential decrease. There is however a spike off to the righthand side that is about 8% larger than the current density on thruster centerline.

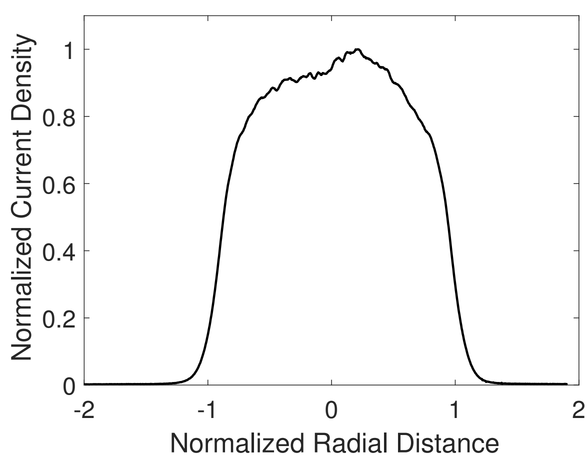

Figure 5: Measured beam current density profile at 3.52 A and 1800 V taken 0.23 r_{t} downstream of the optics.

Superimposed on this central potential dip are large positive spikes that seem to be due to individual beamlets. Past studies with a NEXT thruster have detected 200 individual beamlets at 0.025 r_{t}, noting

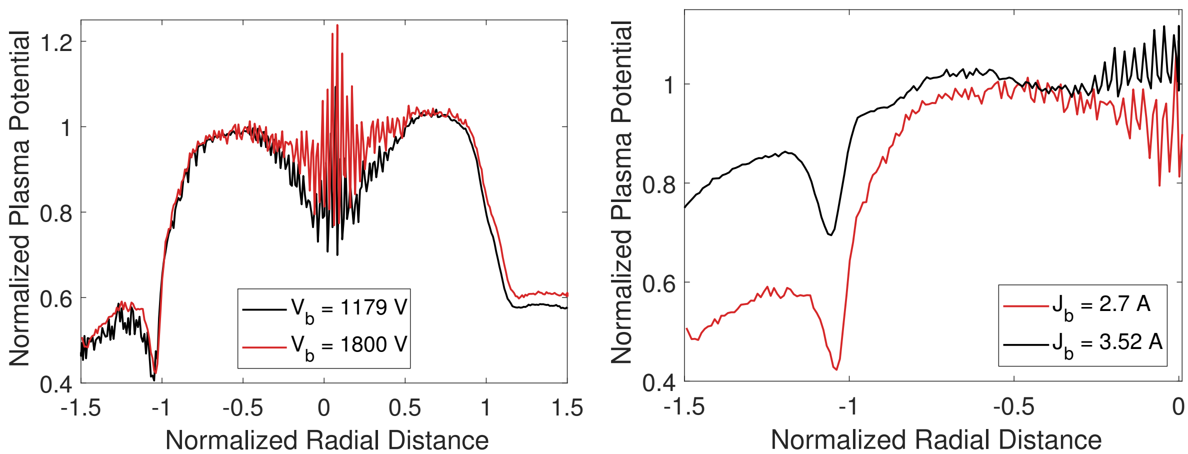

(a) Plasma potential across the front of the thruster as a function of beam voltage.

(b) Plasma potential across the front of the thruster as a function of beam current.

Figure 6: The plasma potential measured radially 0.02 r_t downstream of the acclerator grid for various operating conditions.

that the "merger of beamlets was nearly complete at [0.1 r_t]."[19] The diameter of the emissive probe was coincidentally the same size as the grid apertures. This suggests that it is plausible that the individual spikes are in fact ion beamlets. Between beamlets, the potential is lower, and then within the beamlet the potential increases, leading to the shape in the figure.

The plasma potential as a function of radial distance at different throttle points is presented in Fig. 6. At a constant beam current of 2.7 A, the dip seen on centerline decreases as the beam voltage is increased from 1179 V to 1800 V.

The magnitude of the individual beamlet spikes is larger at the higher beam voltage. At a constant beam voltage of 1800 V, the dip is less prominent at the higher beam current and in fact the potential near the thruster centerline seems to increase slightly over the value at mid-radius. Additionally, off to the side of the thruster the potential does not fall off as steeply at the highest beam current. The data presented in Fig. 6b was taken over two different test segments with a vacuum break in between.

Figures 4 and 6 suggest that charge exchange ions born within a half radius of the thruster centerline will tend to move towards the center of the grids, increasing erosion on centerline relative to larger radii. Also, charge exchange ions that are born near the edge of the beam will see a potential gradient that falls off to the sides of the thruster, in effect protecting the outer apertures and reducing pit and groove erosion at large radii. This agrees with examination of accelerator erosion following two NEXT wear tests, which showed that the apertures near the edge of the grid exhibited less erosion than the central apertures.[20, 21] Results from the 50 000 h long duration test suggested that at the inner radii there was net erosion, which transitioned to net deposition of facility backsputtered carbon at $\sim$0.5 r_t.[21] The beam current density also decreases near the edge of the beam as seen in Fig. 5; therefore, the radial plasma potential profile is merely one possible factor that leads to reduced erosion of the edge apertures.

The plasma potential on the centerline axis at the highest power is plotted in Fig. 7 for two of the probes in the setup. Interestingly, for the fourth emissive probe, the plasma potential rapidly falls off at 0.015 r_t as the probe approaches the accelerator grid, which is at -200 V. However, for the fifth emissive probe the potential actually increases as the probe approaches the accelerator grid. Again, multiple emissive probes were required because their lifetime in the beam was very short, especially at the upper end of the throttle table. The reason for this discrepancy between probes is not completely clear, but figs. 4 and 6 may offer a clue. It is possible to discern individual beamlets at $\leq$0.1 r_t, and these ion beamlets have an increased potential that appears as a spike on the plots. Therefore, it seems that as probe 4 approaches the grids it is between the beamlets and sees the potential of the accelerator grid sheath, whereas probe 5 approaches the grids within a beamlet and sees an increasing potential as the density of ions increases. Each probe was aligned to the center aperture, but there is some uncertainty and small error in the alignment process (on

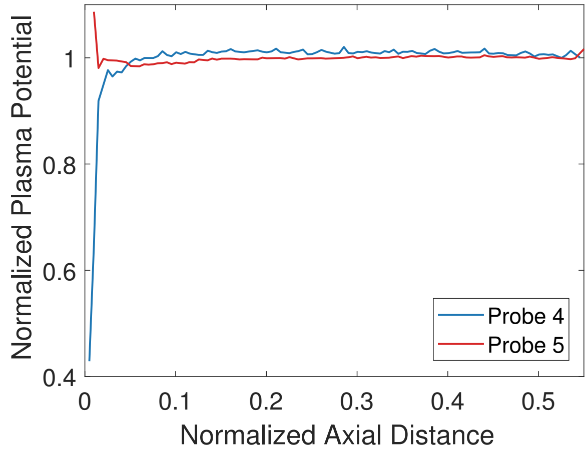

Figure 7: Plasma potential on axis measured at 3.52 A and 1800 V using two different emissive probes.

the order of 1 mm) that appears to manifest very near to the grid.

Axial probe data were taken off thruster centerline at full power, and can be seen in Fig. 8. The increasing distance from the grids as the radial location increases is accounted for, i.e. the sweep at 0.05 r_t gets closer to the thruster than the sweep at 0.25 r_t. Near to the thruster centerline, the potential seems to increase and then decrease rapidly. The reason for this behavior is not clear, but again this may be an effect caused by the probe getting close enough to the thruster to be influenced by individual beamlets. The data shown is taken only as the probe is moving axially towards the thruster, and not when the probe stops, but as the probe nears its closest approach the stage decelerates before reversing direction. While it seems that the plasma potential peak is moving further from the grid surface, notice that the scale in Fig. 8a shows that the location of the peak only changes by 0.005 r_t as the radial location increases from 0.05 to 0.2. The magnitude of the increase in plasma potential mostly decreases as a function of radius. Moving out to mid-radius and beyond the potential remains fairly flat axially.

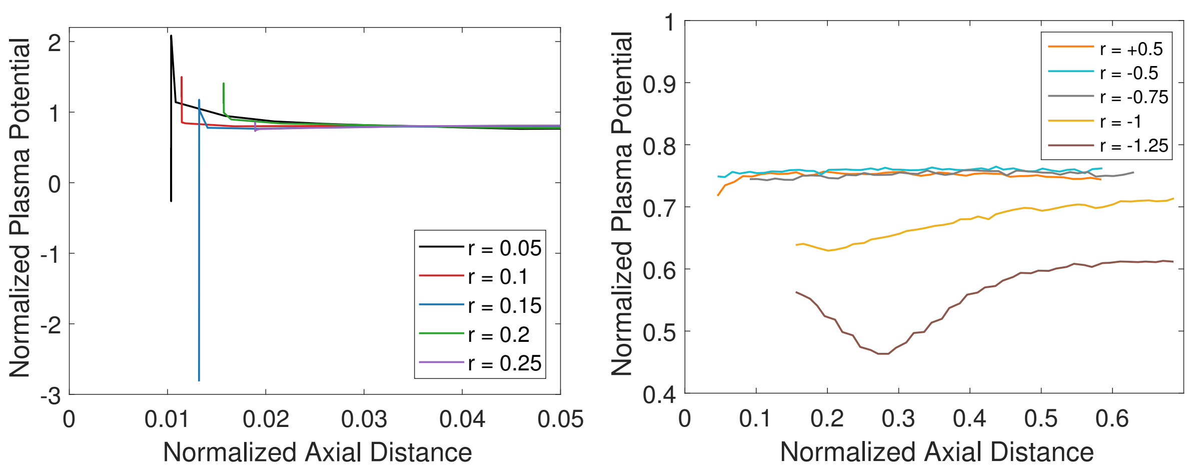

(a) Plasma potential as a function of axial distance at radial positions near the thruster centerline.

(b) Plasma potential as a function of axial distance at large radial positions.

Figure 8: The plasma potential measured axially at various thruster radii.

At the edge of the beam there is a slight dip in the potential, but outside the beam at 1.25 r_t there is a noticeable potential well. Downstream of the thruster at a distance of $\sim$0.7 r_t, the probes are at an angle of approximately 20° with respect to the grid edge and are starting to measure the ion beam. This agrees with past measurements of NEXT's ion beam divergence half-angle.[19,22] The potential decreases as the probes move towards the thruster and the ion density decreases (similar to the profile at 1 r_t). From 0.3 r_t inwards, the potential begins to rise again. The plasma density here is low and mostly comprised of charge-exchange ions, so facility effects may be causing this increase off to the side of the thruster and the associated potential well.

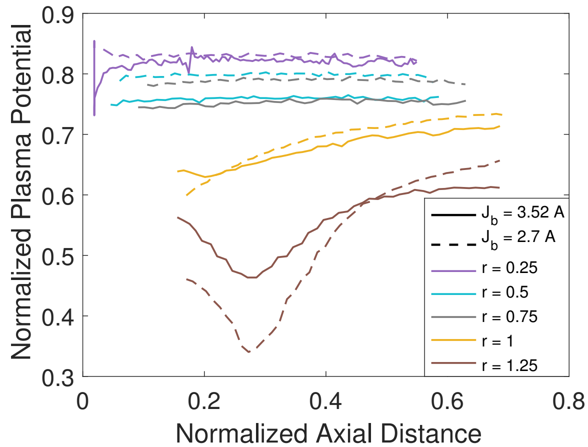

Figure 9: Plasma potential off-axis measured at two different throttle points.

Figure 9 compares the plasma potential off-axis for two different beam currents with a beam voltage of 1800 V. The data at 3.52 A was taken with emissive probe 4 and the data at 2.7 A was taken with emissive probe 5. The general trend across beam currents agrees well. The average plasma potential falls as the radius increases. The potential is fairly flat until the edge of the beam where in both cases the potential decreases as one moves closer to the thruster. Again, outside the beam, the plasma potential exhibits a decrease followed by increase, leaving a small potential well.

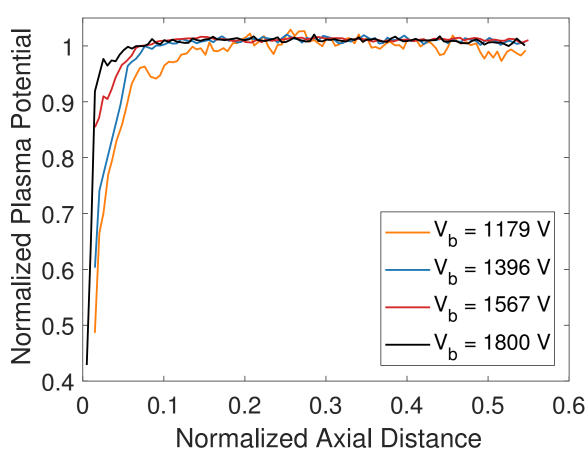

Figure 10: Plasma potential on thruster centerline as a function of beam voltage for a beam current of 3.52 A

For a beam current of 3.52 A, the plasma potential on axis at four different beam voltages is plotted in Fig. 10. At the highest voltage, the drop in plasma potential is nearest to the grids and is the steepest. As the voltage is decreased, the point at which the plasma potential begins to fall off moves further from the grid surface. Kaufman gives the expression for the length to the plane at which the beam becomes neutralized, which is the extent of the accelerator grid sheath and called the deceleration length, in a two-grid thruster as

$$\ell_\mathrm{d} = \ell_\mathrm{a}\sqrt{\frac{1+3\sqrt{R}-4R\sqrt{R}}{F_\mathrm{s}}\frac{j_\mathrm{b}}{j_\mathrm{CL}}} \tag{1}$$

where ℓ_a is the acceleration length (approximately the grid gap), F_s is the open area fraction of the screen grid, j_b is the beam current density, and j_{CL} is the Child-Langmuir limited current density.[23] The value of the R-ratio is

$$R = \frac{V_N}{V_T} \tag{2}$$

where V_T is the total voltage and V_N is the net voltage. The total accelerating voltage is the difference between the beam voltage V_b and the accelerator voltage V_a, $V_T = V_b - V_a$. The net accelerating voltage is $V_N = V_b + V_a$, where V_a is always negative for ion beams. The accelerator voltage is approximately constant and $|V_a| < |V_b|$ for the curves shown in Fig. 10, so the R-ratio increases as the beam voltage increases. The length to the neutralization plane decreases as the R-ratio increases, and equals 0 when $R = 1$. The R-ratio changes by approximately 11% as the beam voltage is increased, and the trend in Fig. 10 agrees qualitatively with the extent of the accelerator sheath predicted by equation (1).

Figures 7–10 show the plasma potential as a function of axial distance. The plots show that potential is fairly flat up to at least 0.2 r_t from the accelerator surface. The beamlets themselves have a potential that increases, but between the beamlets, where the pit and groove erosion occurs, the potential falls steeply near the grid. This suggests that there is no barrier to charge-exchange ions that are created in the plume near the thruster, and that they can easily impact the accelerator grid. The lack of variation in plasma potential agrees with data taken on centerline of an NSTAR thruster, where up to 3 thruster radii from the grid the plasma potential varied by less than 1 V at the highest power.[7] Previous measurements of a NEXT multi-thruster array showed that the plasma potential changed by only 0.5 V over distances from 0.25 to 2.25 r_t.[9]

B. Electron Temperature

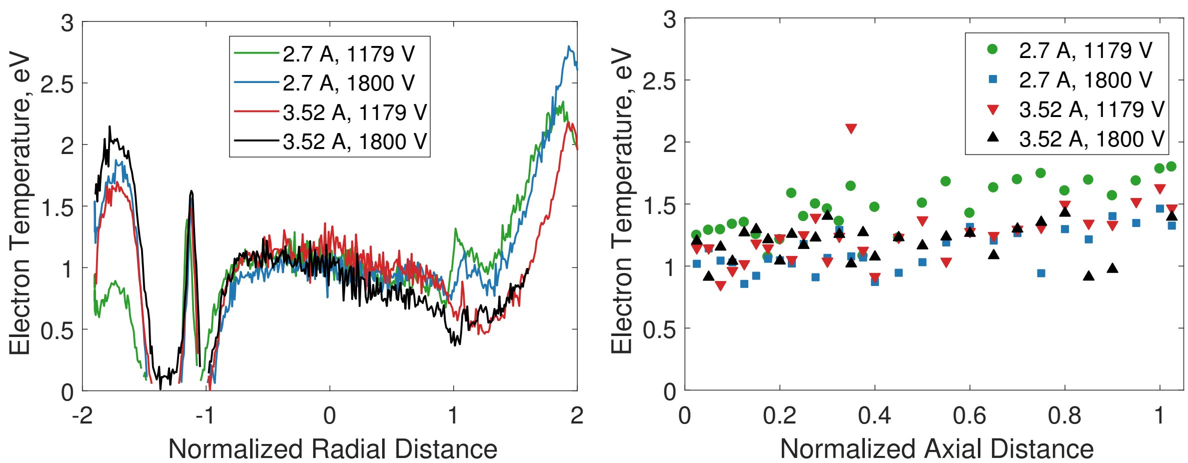

(a) Electron temperature along a radial sweep, 0.025 r_t downstream of the accelerator grid.

(b) Electron temperature moving axially away from the thruster.

Figure 11: The electron temperature in front of the thruster as measured with a triple Langmuir probe.

Figure 11 shows the electron temperature as a function of both axial and radial distances, normalized to the thruster radius. In Fig. 11a, the probe is swept across the face of the thruster, 0.025 r_t downstream of the accelerator grid, and the thruster is between -1 and 1 on the plot. Directly in front of the thruster, the electron temperature remains around 1 eV, and shows no trend with beam current or beam voltage. There is a slight dip towards the right side of the thruster, r = +1, which could be attributed to asymmetries in the beam current profile. Figure 5 shows the measured beam current profile taken 0.23 r_t downstream of the thruster, which shows a slight bump on the right-hand side of the profile.

Outside of the beam, where the plasma density is low, the electron temperature doubles to approximately 2 eV. Outside the ion beam, the electron temperature seems to vary more between power levels. This could be attributed to the fact that there is no plasma source in this area and the data are highly susceptible to noise. Additionally, there is a clear difference in shape between the areas from -2 to -1 and from 1 to 2 that appears in all the scans. It is not obvious why this would be the case, but one possible reason is that the vacuum facility infrastructure is different on each side of the thruster. For instance there is an ion gauge to the right of the thruster (positive radial position in the figures), and there is more mass associated with the probes and their motion stages to the left of the thruster. The structure to each side of the thruster can be seen in Fig. 12. Note that the neutralizer cathode is above the thruster, and not in the plane of the probe sweep.

Figure 12: Photograph of test setup showing the facility infrastructure to each side of the thruster.

A previous study in the plume on an NSTAR thruster measured electron temperatures between 1 and 1.7 eV on centerline.[7] Electron temperature was found to be relatively constant up to 3 thruster radii from the grids. Another study using a NEXT thruster found the electron temperature 0.2 r_t from the grid was between 0.5 and 1.2 eV for all throttle points.[8] Those previous studies show an electron temperature trend with power which is attributed to the fact that the neutralizer coupling voltage changes by more than 2 V and the neutralizer keeper voltage changes by $\gtrsim$1 V. For the data in Fig. 11, the coupling voltage and neutralizer keeper voltage only varied by 0.2 V and 0.7 V respectively. This may explain why near to the thruster the electron temperature is constant with operating power within the experimental error of $\sim$25%. Other NEXT thrusters also exhibit the relatively constant coupling and neutralizer keeper voltage, which are a feature of the most recent NEXT throttle table at high beam currents, >2.7 A. These higher beam currents were the focus of this study, therefore nuances of electron temperature trends at lower throttle points were not analyzed and are left to future work.

C. Ion Density

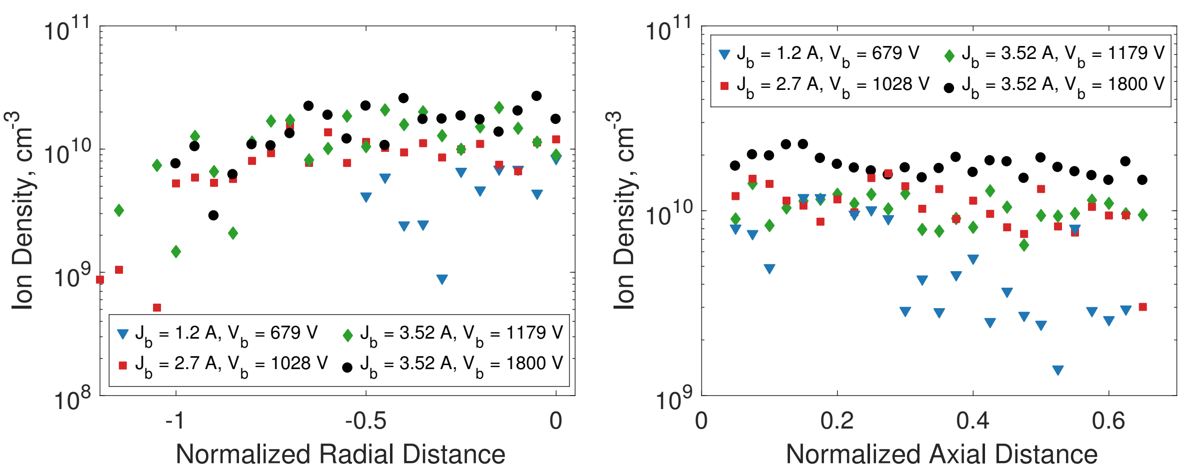

(a) Electron temperature along a radial sweep, 0.025 r_t downstream of the accelerator grid.

(b) Ion density moving axially away from the thruster.

Figure 13: The ion density in front of the thruster as measured with a Langmuir probe.

The ion density downstream of the thruster is measured by operating one collector of the triple Langmuir probe as a single Langmuir probe. The measured ion density at various throttle levels in both the radial and axial direction is shown in Fig. 13. The ion density near to the thruster roughly scales with beam current as expected. As seen in Fig. 13a, moving outside of the ion beam the ion density falls by an order of magnitude. For the three highest powers plotted in Fig. 13b, the ion density remains relatively constant, but for the lowest power the ion density falls off as a function of axial distance. This could be due to the fact that at lower powers the data was more susceptible to noise.

IV. Conclusion

The properties of the ion beam plasma downstream of a NEXT ion thruster were measured using emissive and Langmuir probes. The plasma potential as a function of radius showed a slight decrease at the midpoint of the thruster and then fell off rapidly outside of the ion beam. This suggests that the apertures near the center of the grid will be disproportionately affected by charge-exchange erosion as compared to the edge apertures. While there are several factors that can lead to decreased erosion at the beam periphery (i.e. lower current density), this plasma potential trend agrees with the observations of past 2000 h and 50 000 h wear tests.

Depending on which probe was used, the plasma potential on axis either seemed to increase or decrease as the probe approached the accelerator grid. It appears that the fifth emissive probe was measuring the potential within an ion beamlet, which would tend to increase. On the other hand, the fourth emissive probe measured a decreasing potential which is consistent with the fact that the accelerator is at a large negative potential. The potential near the grid fell off more sharply as the beam voltage was increased at a constant beam current. This agrees with the theoretical extent of the accelerator grid sheath, which is a function of R-ratio. Axial measurements made off-center were relatively flat and agreed across beam currents.

The electron temperature was consistent across throttle points, which was in contrast to past studies. However, for this study, the thruster operated with a very consistent neutralizer coupling voltage and neutralizer keeper voltage, whereas past studies attributed variation in electron temperature to changes in these values. The ion density scaled with beam current as expected, and fell off more rapidly as a function of axial distance for lower beam currents.

The aim of this paper was to experimentally measure the plasma properties, and particularly the plasma potential, very near to the thruster. Previous studies have measured these properties, but not in the proximity achieved here. These results will be fed into modeling efforts that are underway at both NASA's Glenn Research Center and Jet Propulsion Laboratory, which are discussed in companion papers.[12,13]

Acknowledgments

The authors would like to acknowledge the assistance of Kevin McCormick, Tom Bollinger, and Brandon Hale with the test setup. This work was completed as part of the NEXT-C project, which is supported by the Planetary Science Division of the Science Mission Directorate, NASA Headquarters.

References

[1] R. Shastry, D. A. Herman, G. C. Soulas, and M. J. Patterson, "Status of NASA's evolutionary xenon thruster (NEXT) long-duration test as of 50,000 h and 900 kg throughput," in *33rd International Electric Propulsion Conference*, no. IEPC-2013-121, (Washington, D.C.), 2013.

[2] J. T. Yim, G. C. Soulas, R. Shastry, M. Choi, J. A. Mackey, and T. R. Sarver-Verhey, "Update of the NEXT ion thruster service life assessment with post-test correlation to the long duration test," in *35th International Electric Propulsion Conference*, no. IEPC-2017-061, (Atlanta, GA), 2017.

[3] J. L. Van Noord, "Lifetime assessment of the NEXT ion thruster," in *43rd Joint Propulsion Conference*, no. AIAA-2007-5274, (Cincinnati, OH), 2007.

[4] R. E. Wirz, J. R. Anderson, and I. Katz, "Time-dependent erosion of ion optics," *J. Propul. Power*, vol. 27, no. 1, pp. 211–217, 2011.

[5] J. R. Brophy, I. Katz, J. E. Polk, and J. R. Anderson, "Numerical simulations of ion thruster accelerator grid erosion," in *38th AIAA/ASME/SAE/ASEE Joint Propulsion Conference*, no. AIAA-2002-4261, (Fort Lauderdale, FL), 2002.

[6] V. H. Chaplin, J. E. Polk, I. Katz, J. R. Anderson, G. J. Williams, G. C. Soulas, and J. T. Yim, "3D simulations of ion thruster accelerator grid erosion accounting for charge exchange ion space charge," in *Joint Propulsion Conference*, no. AIAA 2018-4812, (Cincinnati, OH), 2018.

[7] J. E. Foster, G. C. Soulas, and M. J. Patterson, "Plume and discharge plasma measurements of an NSTAR-type ion thruster," in *36th AIAA Joint Propulsion Conference and Exhibit*, no. AIAA-2000-3812, (Huntsville, AL), 2000.

[8] H. Kamhawi, G. C. Soulas, and M. J. Patterson, "NEXT ion engine 2000 hour wear test plume and erosion results," in *40th AIAA Joint Propulsion Conference*, no. AIAA-2004-3792, (Fort Lauderdale, FL), 2004.

[9] J. E. Foster, M. Patterson, E. Pencil, H. McEwen, and E. Diaz, "Plasma characteristics measured in the plume of a NEXT multi-thruster array," in *42nd Joint Propulsion Conference and Exhibit*, no. AIAA-2006-5181, (Sacramento, CA), 2006.

[10] J. S. Synder, D. M. Goebel, R. R. Hofer, J. E. Polk, N. C. Wallace, and H. Simpson, "Performance evaluation of the T6 ion engine," *J. Propul. Power*, vol. 28, no. 2, pp. 371–379, 2010.

[11] L. M. Bermúdez and J. B. Jermakian, "Modeling, simulation and validation of the Mo and Mo^+ deposition imparted by the NASA evolutionary xenon thruster (NEXT)," in *35th International Electric Propulsion Conference*, no. IEPC-2017-281, (Atlanta, GA), 2017.

[12] J. T. Yim, G. J. Williams, G. C. Soulas, R. Shastry, V. Chaplin, and J. E. Polk, "Uncertainty quantification of modeled electron backstreaming failure for the NEXT ion thruster," in *36th International Electric Propulsion Conference*, no. IEPC-2019-722, (Vienna, Austria), 2019.

[13] J. E. Polk, V. Chaplin, J. Kellan, J. T. Yim, G. C. Soulas, G. J. Williams, and R. Shastry, "Modeling ion optics erosion in the NEXT ion thruster using the CEX2D and CEX3D codes," in *36th International Electric Propulsion Conference*, no. IEPC-2019-907, (Vienna, Austria), 2019.

[14] J. P. Sheehan and N. Hershkowitz, "Emissive probes," *Plasma Sources Sci. Technol.*, vol. 20, no. 063001, 2011.

[15] J. P. Sheehan, Y. Raitses, N. Hershkowitz, I. Kaganovich, and N. Fisch, "A comparison of emissive probe techniques for electric potential measurements in a complex plasma," *Phys. Plasmas*, vol. 18, no. 7, p. 073501, 2011.

[16] F. F. Chen, J. D. Evans, and W. Zawalski, *Electric Probes*, pp. 113–200. New York: Academic Press, 1965.

[17] N. Hershkowitz, *How Langmuir Probes Work*, pp. 113–183. San Diego: Academic Press, 1989.

[18] B. E. Cherrington, "The use of electrostatic probes for plasma diagnostics–a review," *Plasma Chem. Plasma Process.*, vol. 2, no. 2, pp. 113–140, 1982.

[19] J. E. Pollard, K. D. Diamant, M. W. Crofton, M. J. Patterson, and G. C. Soulas, "Spatially-resolved beam current and charge-state distributions for the NEXT ion engine," in *46th AIAA/ASME/SAE/ASEE Joint Propulsion Conference & Exhibit*, no. AIAA-2010-6779, (Nashville, TN), 2010.

[20] G. C. Soulas, H. Kamhawi, M. J. Patterson, M. A. Britton, and M. M. Frandina, "NEXT ion engine 2000 hour wear test results," in *40th Joint Propulsion Conference and Exhibit*, no. AIAA-2004-3791, (Fort Lauderdale, FL), 2004.

[21] G. C. Soulas and R. Shastry, "Post-test examination of NASA's evolutionary xenon thruster long-duration test hardware: Ion optics," in *52nd AIAA/SAE/ASEE Joint Propulsion Conference*, no. AIAA-2016-4632, (Salt Lake City, UT), 2016.

[22] D. A. Herman, G. C. Soulas, and M. J. Patterson, "Performance evaluation of the prototype model NEXT ion thruster," in *43rd Joint Propulsion Conference*, no. AIAA-2007-5212, (Cincinnati, OH), 2007.

[23] H. R. Kaufman, "Technology of electron-bombardment ion thrusters," in *Advances in Electronics and Electron Physics*, vol. 36, pp. 265–373, New York: Academic Press, 1975.